26th IMEKO TC4 International Symposium
24rd International Workshop on ADC and DAC Modelling and Testing
IMEKO TC-4 2023
Pordenone, Italy / September 20-21, 2023

A simple and accurate resistance comparator with a long-scale ratiometric digital multimeter

Martina Marzano[1], Vincenzo D'Elia[1], Massimo Ortolano[2], Luca Callegaro[1]

[1]*INRIM Istituto Nazionale di Ricerca Metrologica, Torino, Italy, m.marzano@inrim.it*
[2]*Politecnico di Torino, Torino, Italy*

***Abstract* – This paper describes a resistance comparator, based on a long-scale digital multimeter, suitable for primary resistance metrology. The comparator measures the resistance ratio between two four-terminal standards from the readings of the multimeter, when operating in the voltage ratio mode. The quasi-simultaneous measurement of the resistors voltages strongly relaxes the stability requirements of the driving current source with respect to other published comparators, which are based on a shuttling voltage reading. Measurements between resistors of nominal value $12\,906\,\Omega$ (the quantized Hall resistance) agree with a reference value, given by a dc current comparator bridge, within a few parts in 10^8.**

I. INTRODUCTION

Accurate resistance comparators operating with resistances of a few kiloohms are key instruments for the realization of the ohm from the quantum Hall effect (QHE) in dc, and for its dissemination from National Metrology Institutes (NMIs) to calibration laboratories.

Resistance comparators based on the potentiometric method [1,2] were developed soon after the discovery of the QHE. In this type of instrument, the voltages across the two series-connected resistors under comparison are measured by difference against a fixed compensation voltage, and the resistance ratio is determined from the voltage ratio. If the difference between the two voltages across the resistors and the compensation voltage is small, the difference voltmeter loading on the potentiometer circuit is negligible and its accuracy need not to be tight. Although simple in principle, the implementation of the potentiometric method requires high-isolation switches and stable sources of voltage and current. In fact, the compensation voltage source and the current source should be stable over the time scale of the two readings, which can be of several minutes.

In subsequent years, for primary resistance metrology applications, many NMIs replaced potentiometric resistance comparators with current comparator bridges, operating either at room or at cryogenic temperature. Current comparator bridges, now commercially available, are state-of the-art instruments delivering the best accuracy to date. However, the emergence in recent years of quantum Hall resistance standards based on novel materials, such as graphene, operating in less demanding conditions than their gallium arsenide counterparts, has revived the interest in simpler and less expensive instruments which can possibly be used routinely in diverse metrological applications.

The potentiometric approach was simplified in the 1990s with the use of long-scale digital multimeters (DMMs) performing direct measurements of the two voltages across the resistances under comparison [3-7]. Stable compensation sources are no longer necessary, but stable current sources and high-isolation reversal switches are still needed.

In [8] we presented a preliminary version of a comparator based on a ratiometric DMM operating at $1:1$ resistance ratios which further simplifies the approach of [3-7]. Since a ratiometric DMM determines the ratio of the voltage at the input terminals to that at the sense terminals by internally switching in quick succession between these two pairs of terminals, the stability requirements for the current source are less demanding and the imperfect isolation of the switches is possibly compensated by the autozero feature of the DMM. Furthermore, the measurement process can be semiautomated with a minimum of external components. Here we describe an improved version of the comparator which can operate from $1:1$ to about $10:1$ resistance ratios and which is equipped with a programmable current source for more flexibility. One or both the resistors under comparison can be quantum Hall resistance standards.

II. RESISTANCE COMPARATOR SETUP

The schematic diagram of the proposed resistance comparator setup is shown in Fig. 1.

The core of the measuring system is a long-scale ratiometric DMM. We used a Keysight 3458A, but other models capable of ratiometric operation should work as well.

The two resistors under comparison are R_1 and R_2, both defined as four-terminal standards and connected in series at the low current terminals IL1 and IL2. A current source with floating output drives the two resistors with a current I at the high current terminals IH1 and IH2. We tested two different sources: a low-noise battery-operated fixed current bespoke source (described in [8] and here adapted to operate at different resistance ratios), and a commercial programmable current source (Adret Electronique 103A),

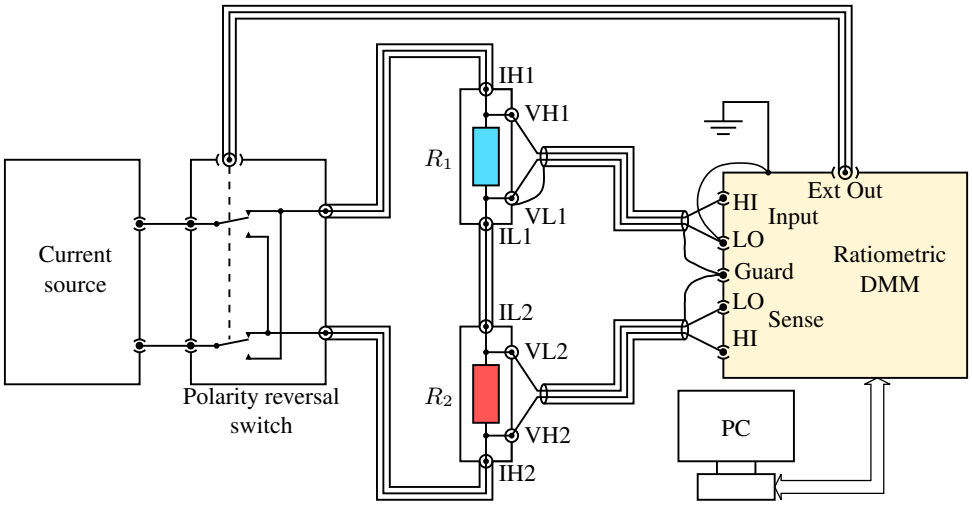

Fig. 1. Schematic diagram of the comparator. The resistors R_1 and R_2 are connected in the forward *configuration.*

which adds flexibility to the setup. To cancel the DMM gain error, the resistors R_1 and R_2 are successively connected to the DMM in two mirroring configurations, labelled *forward* and *reverse* in the following. In the forward configuration, as shown in Fig. 1, the voltage terminals VH1 and VL1 of R_1 are connected to the DMM input HI and LO terminals, respectively, and the voltage terminals VH2 and VL2 of R_2 are connected to the DMM sense HI and LO terminals, respectively. In the reverse configuration, R_1 is connected to the sense terminals and R_2 to the input terminals. The system is grounded at the DMM LO terminals to avoid any error from the common-mode input resistance[1].

To cancel the errors caused by offsets, thermoelectric voltages and bias currents, the polarity reversal switch periodically reverses the direction of I. The operation of this switch is controlled, through a driver, by the Ext Out signal generated by the DMM.

The computer PC controls the DMM and the polarity reversal switch via an IEEE-488 communication interface.

III. OPERATION AND MEASUREMENT MODEL

The operation of the resistance comparator is as follows. The system is first set in the forward configuration, and $2M \times N$ voltage ratio readings $Q^{\mathrm{F}+}_{k,j}$ and $Q^{\mathrm{F}-}_{k,j}$, $j = 1, \ldots, M$ and $k = 1, \ldots, N$, are taken by periodically reversing the current I every M readings; then the comparator is manually set in the reverse configuration, and other $2M \times N$ voltage ratio readings $Q^{\mathrm{R}+}_{k,j}$ and $Q^{\mathrm{R}-}_{k,j}$ are taken. Owing to the operation of the DMM, this measurement sequence is different from the one commonly used in other works [2, 4, 7], where the current is reversed at each voltage measurement. Once the measurement is completed, each group of M readings is averaged to yield the following sequence of average ratios[2] (with $\mathrm{X} = \mathrm{F}, \mathrm{R}$): $Q^{\mathrm{X}\pm}_k = M^{-1} \sum_{j=1}^{M} Q^{\mathrm{X}\pm}_{k,j}$; $Q^{\mathrm{X}}_k = (Q^{\mathrm{X}+}_k + Q^{\mathrm{X}-}_k)/2$; and $Q^{\mathrm{X}} = N^{-1} \sum_{k=1}^{N} Q^{\mathrm{X}}_k$. From Q^{F} and Q^{R}, the comparator reading can be obtained as

$$Q = \sqrt{\frac{Q^{\mathrm{F}}}{Q^{\mathrm{R}}}}. \tag{1}$$

Taking into account the sources of uncertainty described in the comprehensive analysis of [4], and assuming that the input and sense ranges do not change between the forward and reverse configurations[3], the measurement model can be approximated as

$$Q = \frac{R_1}{R_2}\left[1 + \epsilon + \frac{1}{2}(R_2 - R_1)(G_{\mathrm{I}} + G_{\mathrm{S}})\right], \tag{2}$$

where ϵ is the relative error due to the DMM's differential nonlinearity and transfer uncertainty between the forward and reverse configurations, and G_{I} and G_{S} are the leakage conductances at the DMM's input and sense terminals, respectively, averaged across the measurement steps and including the leakage conductances of the current source and the switch. When $R_1 \approx R_2$, the correction terms are minimized. We expect the effect of the feed-through

[1] According to the Keysight 3458A's specifications [9], for a proper operation, the voltage between the input and sense LO terminals should not exceed 0.25 V. This limitation should not cause any issue in most practical cases.

[2] It is indeed possible to compute Q^{F} and Q^{R} directly, without computing intermediate averages first, but the sequence described above allows one to analyze the stability of the measurements as reported in Sec. IV.

[3] It turns out [9] that even if it's possible to disable the input autoranging function of the Keysight 3458A, the sense autoranging function cannot be disabled. Therefore, keeping the same ranges between the forward and reverse configurations requires some caution, and might limit the range of ratios that can be measured with the best accuracy.

of the DMM's internal switches to be cancelled by its autozero mechanism, but further investigation may be needed to confirm this hypothesis.

IV. EXPERIMENTAL RESULTS

The comparator has been mainly tested at $1:1$ ratios with two $12\,906\,\Omega$ resistors: R_1 is a Vishay HZ series resistor thermally insulated in a polystyrene box; R_2 is a Vishay H series VHA resistor equipped with a standalone thermostat at $29\,^\circ\mathrm{C}$. The difference between the two resistances is about $0.3\,\Omega$. The results from the comparator were validated against reference measurements obtained by a direct current comparator bridge (DCC bridge, Measurement International AccuBridge 6010D). The DCC bridge measured in succession the ratios R_1/R_{pivot} and R_2/R_{pivot}, where R_{pivot} is a $1\,\mathrm{k}\Omega$ thermostatted resistance standard, and these two ratios were then combined to obtain a reference ratio Q^{ref}. Tests at different resistance ratios are being made, but the analysis of the results has not been completed yet.

Fig. 2 shows two example measurements at $1:1$ ratio. The first five ratio measurements after each polarity reversal are discarded and not reported in the figure. The measurement reported in Fig. 2(a), for which $M = 25$ and $N = 20$, was performed with the battery-operated bespoke current source [8] set to $I = 30\,\mu\mathrm{A}$; the measurement reported in Fig. 2(b), for which $M = 25$ and $N = 15$, was instead performed with the programmable current source set to $I = 50\,\mu\mathrm{A}$. The DMM integration time was set to $2\,\mathrm{s}$ (100 power line cycles) and the duration of each ratio measurement was about $8\,\mathrm{s}$, that is, $4\,\mathrm{s}$ for each voltage. Fig. 3 reports the Allan deviation of the measurements of Fig. 2 as a function of the integration time τ, separately for the forward and reverse configurations. It can be argued that the noise level of the programmable current source is on the average slightly higher than that of the battery-operated source, but not in a significant way.

Tab. 1 reports the uncertainty budgets for the measurements of Fig. 2. The type A uncertainty components were evaluated from the extrapolated Allan deviation at the actual measurement time. The input and sense resistances were determined by adapting the method described in [10] to the ratiometric operation of the DMM, yielding $R_{\mathrm{I}} \approx 540\,\mathrm{G}\Omega$ and $R_{\mathrm{S}} \approx 2\,\mathrm{T}\Omega$. This values do not include the leakage conductances of the current source, and further characterizations need to be performed for resistance ratios different from $1:1$. The error term ϵ which appears in (2) has been considered negligible for a $1:1$ ratio, but also in this case further characterizations are needed to confirm this hypothesis.

Tab. 2 reports the comparison between the results obtained from the measurements of Fig. 2 and those obtained from the DCC. The reported uncertainty for the DCC is the type A uncertainty component evaluated from the Al-

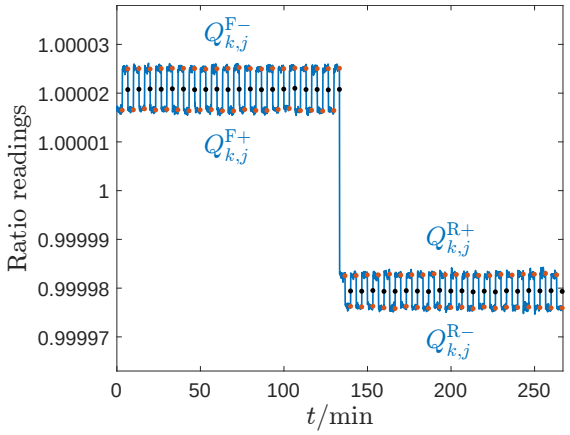

(a)

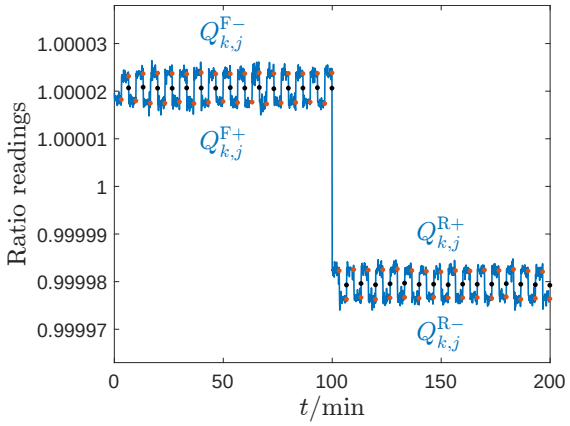

(b)

Fig. 2. Time series of the comparator readings when measuring two $12\,906\,\Omega$ resistors: (a) measurement with the bespoke current source with $I = 30\,\mu\mathrm{A}$, $M = 25$ and $N = 20$; (b) measurement with the programmable current source with $I = 50\,\mu\mathrm{A}$, $M = 25$ and $N = 15$. The blue lines (—) represent the individual ratio readings $Q^{\mathrm{F}+}_{k,j}$, $Q^{\mathrm{F}-}_{k,j}$, $Q^{\mathrm{R}+}_{k,j}$ and $Q^{\mathrm{R}-}_{k,j}$; the red bullets (•) represent the averages over M points $Q^{\mathrm{F}+}_{k}$, $Q^{\mathrm{F}-}_{k}$, $Q^{\mathrm{R}+}_{k}$ and $Q^{\mathrm{R}-}_{k}$; and the black bullets (•) represent the forward and reverse averages Q^{F}_{k} and Q^{R}_{k}. The periodic oscillations correspond to current reversal events; the large step in the middle is the switching from the forward to the reverse configuration.

Table 1. Uncertainty budgets for the measurements of Fig. 2

i	Quantity	Type	$u_i(Q)/(\mathrm{n}\Omega\,\Omega^{-1})$ Fig. 2(a)	Fig. 2(b)
1	Q^{F}	A	8.1	11
2	Q^{R}	A	10.9	12
3	G_{I}	B	< 0.1	< 0.1
4	G_{S}	B	< 0.1	< 0.1
	Q	RSS	14	16

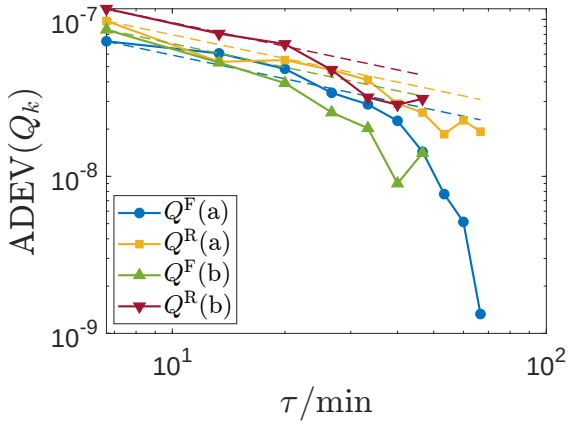

Fig. 3. Allan deviations of the measurements of Fig. 2 vs. the integration time τ: the blue line with circle markers represents the Allan deviation of the Q_k^{F}'s of Fig. 2(a); the yellow line with square markers represents the Allan deviation of the Q_k^{R}'s of Fig. 2(b); the green line with upward-pointing triangle markers represents the Allan deviation of the Q_k^{F}'s of Fig. 2(b); and the red line with downward-pointing triangle markers represents the Allan deviation of the Q_k^{R}'s of Fig. 2(b). The dashed lines represent the Allan deviation extrapolated for white noise time series.

Table 2. Comparison between the measurements of Fig. 2 and the reference measurements determined by the DCC.

Meas.	$\frac{Q-1}{\mu\Omega\,\Omega^{-1}}$	$\frac{Q^{\mathrm{DCC}}-1}{\mu\Omega\,\Omega^{-1}}$	$\frac{Q-Q^{\mathrm{DCC}}}{\mathrm{n}\Omega\,\Omega^{-1}}$
(a)	20.697(14)	20.692(21)	5(25)
(b)	20.609(19)	20.632(25)	−22(31)

lan deviation of the measurements. As can be seen from Tab. 2, the results are compatible within the standard uncertainty.

V. CONCLUSIONS AND PERSPECTIVES

The resistance comparator herewith presented allows one to measure the resistance ratio between two four-terminal resistors in a simple and automated way. The multimeter employed is available in any metrology laboratory, and the additional components required (current source, switch) are not critical. The measurements reported show that the comparator, when performing $1:1$ ratio measurements at the quantized Hall resistance level, match those of a top-of-the-line current comparator bridge, with comparable uncertainty. The comparator is now being characterised for measurements with other resistance ratio values, for which the linearity of the DMM can play a significant role. We will report about the characterisation outcome at the Conference.

VI. ACKNOWLEDGMENT

This work has been supported by the project CAPSTAN *Quantum electrical Italian national capacitance standard* funded by the MIUR *Progetti di Ricerca di Rilevante Interesse Nazionale* (PRIN) Bando 2020, grant 2020A2M33J.

REFERENCES

[1] L. Bliek, E. Braun, F. Melchert, P. Warnecke, W. Schlapp, G. Weimann, K. Ploog, G. Ebert, and G. E. Dorda, "High precision measurements of the quantized Hall resistance at the PTB," *IEE Proc. Sci. Meas. Tech.*, vol. IM-34, no. 2, pp. 304–305, 1985.

[2] G. Marullo Reedtz and M. E. Cage, "An automated potentiometric system for precision measurement of the quantized Hall resistance," *J. Res. Natl. Bur. Std*, vol. 92, no. 5, pp. 303–310, 1987.

[3] M. E. Cage, D. Yu, B. M. Jeckelmann, R. L. Steiner, and R. V. Duncan, "Investigating the use of multimeters to measure quantized Hall resistance standards," *IEEE Trans. Instr. Meas.*, vol. 40, no. 2, pp. 262–266, 1991.

[4] K. C. Lee, M. E. Cage, and P. S. Rowe, "Sources of uncertainty in a DVM-based measurement system for a quantized Hall resistance standard," *J. Res. Natl. Inst. Stand. Technol.*, vol. 99, no. 3, pp. 227–240, May-June 1994.

[5] G. Rietveld and F. P. Jans, "A DVM-based accurate measurement setup for QHE resistance measurements," in *1998 Conference on Precision Electromagnetic Measurements Digest*, Washington DC, USA, 1998, pp. 416–417.

[6] C. Rietveld and C. J. Van Mullem, "Uncertainty analysis of a DVM-based quantum Hall measurement set-up," in *Conference on Precision Electromagnetic Measurements Digest CPEM 2000*, Sydney, NSW, Australia, 2000, pp. 90–91.

[7] P. Svoboda, P. Chrobok, and P. Vašek, "A simple DMM-based measuring system for QHE resistance measurements," in *2000 Conference on Precision Electromagnetic Measurements (CPEM 2000)*, Sydney, NSW, Australia, 2000, pp. 566–567.

[8] M. Marzano, V. D'Elia, M. Ortolano, and L. Callegaro, "A resistance comparator based on a long-scale digital voltmeter," in *2022 Conference on Precision Electromagnetic Measurements (CPEM 2022)*, Wellington, New Zealand, 2022, pp. 1–2.

[9] Keysight, "3458A multimeter data sheet," Oct. 2021.

[10] G. Rietveld, "Accurate determination of the input impedance of digital voltmeters," *IEE Proc. Sci. Meas. Tech.*, vol. 151, no. 5, pp. 381–383, 2004.